Supporting Information

Kelsch *et al.* 10.1073/pnas.0807970105

SI Text

Retroviral Delivery of PSD-95:GFP to Cultured Neurons. We determined whether retroviral delivery of PSD-95:GFP could serve as an appropriate marker for postsynaptic sites. PSD$^+$Cs were contacted by the presynaptic marker bassoon (Fig. S1*C*), and endogenous and exogenous PSD-95 overlapped in clusters (Fig. S1*D*), further supporting the idea that PSD-95:GFP could be used as a postsynaptic marker.

We also tested whether the delivery of PSD-95:GFP via retroviral vectors could result in confounding effects on synaptic development. It has been reported in cultured hippocampal neurons that 5- to 10-fold overexpression of PSD-95 by transient transfection led to strengthening or increase in the number of AMPA receptor-mediated mEPSCs (1). Our experiments revealed that the modest level of expression achieved with retroviral expression (Fig. S1*E*) did not change the strength or number of AMPA receptor-mediated mEPSCs *in vitro* (Fig. S1 *F* and *G*).

Synaptic Glutamatergic Input to Different GC Domains. Two recent studies (2, 3) observed that the synaptic glutamatergic input to GCs in the external plexiform layer (distal domain of the apical dendrite) was mediated by a different type of glutamate receptor than that in the granule cell layer (comprising both the basal dendrite and the proximal domain of the apical dendrite) (Fig. S1). It thus remained unclear whether both the proximal domain and the basal dendrite (= basal domain) receive glutamatergic input (2–5). We performed targeted whole-cell recordings of GFP-labeled GCs combined with fluorescence-guided low amplitude stimulation to activate only one or few axonal fibers terminating at a dendritic branch to test for glutamatergic input to the basal and/or proximal domain of postnatal-generated GCs (Fig. S1*A*). We observed faster decay time at the basal and proximal domains than at the distal domain (Fig. S1*B*) in line with previous studies (2, 3). Postsynaptic currents (PSCs) evoked at the basal and proximal domains were both sensitive to the AMPA-receptor modulator cyclothiazide (CTZ, 10 μM) (Fig. S1*B*). These observations suggest that both the basal and proximal domains receive glutamatergic synaptic input.

Synaptic Development of GCs with Dendritic Targeting in the Deep or Superficial Laminae of the External Plexiform Layer (EPL). We had shown that distinct precursors exist for GCs with deep and superficial dendritic targeting in the EPL (9). The dendrites of GCs target with their branches either the deep or superficial laminae of the EPL. GCs with superficial dendritic targeting in the EPL are thought to be connected to tufted cells, whereas GCs with deep dendritic targeting in the EPL contact mitral cells (6). We therefore investigated whether GCs did not only have different dynamics in their synaptic development depending on whether they were born in neonatal or adult animals, but also because they had different dendritic targeting (Fig. 3 and Fig. S2). In adult-born neurons the synaptic development of the proximal dendritic domain preceded the distal domain regardless of whether GCs had deep or superficial targeting. In neonatal-generated GCs, synapse development was simultaneous in the proximal and distal dendritic domains, regardless their dendritic targeting. We performed a three-way ANOVA to examine the effects of the factors deep-/superficial dendritic targeting, dendritic domain, and time of maturation on PSD$^+$C density of GC. There was no interaction between the three factors for adult-born neurons [F (8, 396) = 1.49, P = 0.157] or for neonatal-born neurons [F (8, 396) = 0.24, P = 0.984]. Similarly for Syp$^+$Cs, the synaptic development was independent of whether GCs had deep or superficial dendritic targeting both for neonatal-born GCs [F (3, 212) = 0.67, P = 0.571] or for adult-born GCs [F (3, 212) = 0.30, P = 0.825] (Fig. S3). Thus, this observation and more detailed analysis (data not shown) revealed no significant differences in the development of synapses between GCs with deep or superficial targeting. Further statistical analysis is therefore only shown for the synaptic development of GCs with superficial dendritic targeting (Figs. 3 and 4).

Statistical Analysis of Synaptic Development in GCs with Superficial Dendritic Targeting. We performed a three-way ANOVA with between-subjects comparisons to examine the effects of the factors adult-/neonatal-born, dendritic domain and time of maturation on PSD$^+$C density. There was a significant interaction between the three factors [F (8, 396) = 4.96, $P < 0.001$]. Looking separately at the different dendritic domains, there was a significant interaction between the factors adult-/neonatal-born and time of maturation for the basal domain [F (4, 396) = 2.97, $P < 0.019$], the proximal domain [F (4, 396) = 3.26, $P < 0.012$], and the distal domain [F (4, 396) = 14.38, $P < 0.001$]. We then examined the simple effects comparing adult- and neonatal-born neurons for single time points of maturation in the respective domain. In the distal domain adult-born neurons had significantly lower PSD$^+$C densities than neonatal-born cells at 17 d.p.i. [F (1, 396) = 22.87, $P < 0.001$] and 21 d.p.i. [F (1, 396) = 13.87, $P < 0.001$]. In contrast, in the proximal domain, PSD$^+$C density was consistently higher in the adult- than in the neonatal-born GCs [14 d.p.i.: F (1, 396) = 40.83, $P < 0.001$; 17 d.p.i.: F (1, 396) = 90.40, $P < 0.001$; 21 d.p.i.: F (1, 396) = 105.1, $P < 0.001$; 28 d.p.i.: F (1, 396) = 74.02, $P < 0.001$; 56 d.p.i.: F (1, 396) = 81.60, $P < 0.001$; compare Fig. 3 *A* and *C*]. Finally, in the basal domain that developed PSD$^+$Cs relatively late, the only significant difference was at 56 d.p.i. where adult-born GCs had a higher density [F (1, 396) = 5.60, P = 0.018].

We then performed a three-way ANOVA to examine the effects of the factors adult-/neonatal-born, pre- or postsynaptic marker (PSD$^+$Cs and Syp$^+$Cs in the distal domain), and time of maturation on synapse density. There was no interaction between the three factors [F (3, 212) = 1.64, $P < 0.181$]. Neither the factor presynaptic/postsynaptic marker nor any interaction involving this factor was significant. Therefore, the effects observed in the presynaptic development paralleled the timing of maturation of PSD$^+$C density. In summary, adult-generated GCs have a delayed maturation of synapses in the distal dendritic domain as compared with the proximal domain, whereas GCs generated in the neonatal period develop synapses synchronously in their proximal and distal dendritic domain.

Mean Values of the Length of the Unbranched Segment of the Apical Dendrite. To determine whether differences in the geometry of adult- vs. neonatal-born neurons would be associated with different input synapse densities in the proximal domain, we measured the mean length of the unbranched segment of the apical dendrite. The mean values were 223.3 ± 8.6 μm (n = 105), 208.3 ± 6.2 μm (n = 274), 246.7 ± 7.0 μm (n = 235), and 211.3 ± 8.8 μm (n = 150) for superficial and deep adult-born and superficial and deep neonatal-born GCs, respectively [dendritic length was stereologically measured as described (9). from a sample of 10 tissue sections for each condition, n = 764 GCs at

28 d.p.i.]. There was no significant interaction between the factors deep-superficial targeting and neonatal-/adult-born GCs [F (1, 760) = 1.60, P = 0.207], no difference on the level of the factor neonatal-/adult-born GCs [F (1, 760) = 2.68, P = 0.102; two-way ANOVA].

Materials and Methods

Stereotaxic Injections. Injections of retroviral vectors were performed stereotactically on CD1 mice and SD rats of either sex (Charles River). Neonatal animals were postnatal day 5 and adult animals >56 days old at the time of injection. We infected the progenitors of GCs by injecting an oncoretrovirus into the subventricular zone. Oncoretroviruses have a half-life of approximately six hours (7) at body temperature and infect only actively dividing cells. Because the transient amplifying cell population is the most abundant dividing cell type in the SVZ and the direct precursor to immature GCs, oncoretroviral infection is very effective for birthdating a single cohort of immature neurons (8). Adult mice were only used in initial comparisons of lentiviral vs. oncorteroviral expression of PSD-95:GFP *in vivo* (see also Fig. S4*A*). All subsequent experiments were performed in rats. Adult animals were anesthetized by an i.p. injection of ketamine/xylazine and neonatal animals by hypothermia. Approximately 200 nl of a retroviral stock solution was injected bilaterally into the SVZ (coordinates relative to Bregma: AP 1 mm, L ± 0.9 mm, V 2.3 mm for adult mice; AP 1.2 mm, L ± 1.6 mm, V 3.3 mm for adult rats; AP 0.9 mm, L ± 2.1 mm, V 2.1 mm or AP −0.6 mm, L ± 2.7 mm, V 2.6 mm for neonatal rats) (AP = anterior–posterior, L = lateral, V = ventral).

Neuronal Culture. All experiments were approved by the local Animal Welfare Committee. Embryonic day 17 hippocampi from Sprague–Drawley (SD) rats were dissected in Hank' balanced salt solution (HBSS, Invitrogen) containing $MgCl_2$ and Hepes (Sigma) and digested with papain (Worthington). Papain was inactivated by ovomucoid (Worthington) and the tissue was dissociated in culture medium [Neurobasal medium containing B27 supplement, penicillin, streptomycin, and glutamine (Invitrogen)]. Cells were infected with the lentiviral vector HsynPSD95g and plated at a density of 150,000 cells per ml medium on coverslips coated with polyD-lysine (Sigma) and laminin (Invitrogen). Culture medium was exchanged after 24 h and subsequently changed twice a week. Cultured hippocampal neurons (21 days in culture) were fixed for 15 min in 3% paraformaldehyde and incubated with primary mouse anti-Bassoon antibody (1:750, SySy) or guinea pig anti-PSD-95 antibody (1:400, gift of M. Sheng) in blocking solution containing 0.2% gelatin and 0.3% Triton X-100 in PBS at 4°C overnight. Cultured neurons were then incubated with secondary antibodies (1:750, Alexa Fluor 555, Invitrogen) at 20°C for 90 min.

***In Vitro* Recordings.** Initially we tested olfactory bulb cultures that showed a high frequency of mIPSCs, but only rare mEPSC events. Because of this limitation, we used cultured hippocampal neurons that displayed a higher mEPSC frequency. Recordings were performed at room temperature (22–25°C) in whole-cell voltage-clamp configuration with a patch-clamp amplifier Multiclamp 700B (Axon Instruments). The composition of the extracellular solution was (in mM): 145 NaCl, 5 KCl, 3 $CaCl_2$, 2 $MgCl_2$, 10 glucose, and 10 Hepes, pH 7.3. Composition of the patch pipette solution was (in mM): 2 NaCl, 4 KCl, 130 K-gluconate, 0.25 $CaCl_2$, 0.5 $MgCl_2$, 10 glucose, 10 Hepes, 10 phosphocreatine, 4 Mg-ATP, 0.3 Tris-GTP, and 0.05% Lucifer yellow, pH 7.3. All experiments were performed in presence of 1.5 μM tetrodotoxin (Alomone Labs) and 20 μM biccuculine (Sigma).

mEPSCs were recorded at V_H = −70mV. All mPSCs were reversibly blocked by 10 μM 6,7-dinitroquinoxaline-2,3-dione (DNQX), a reversible AMPA receptor antagonist (data not shown), suggesting that we recorded AMPA receptor-mediated mEPSCs. For control experiments, coverslips from littermate cultures were used and recorded under the same conditions on the same day as neurons infected with HsynPSD95g. Access resistances ranged between 10 and 15 MΩ and were routinely checked during the recording. Recordings were started >5 min. after the whole-cell configuration was established. Continuous traces of mEPSCs were recorded for 10 min. Data were filtered at 1.3 kHz with a four-pole Bessel filter and acquired with pClamp9 (Axon Instruments). 2 or 10 min traces of mEPSCs were analyzed manually with the Mini Analysis Program (Synaptosoft) for high and low frequency of mEPSCs, respectively. Statistic analyses of data are reported as mean ± SEM. Lucifer yellow-filled neurons were stained against GAD-65 (Chemicon) and only GAD-65-negative cells were selected (data not shown) as they had shown the strongest potentiation of synapse strength and number in hippocampal culture (1).

Brain Slice Recordings. Rat pups were bilaterally injected with 1 μl oncoretroviral vector (MRSVPalmG) expressing palmitoylated GFP in aSVZ or pSVZ in neonatal rats. At 21 to 23 d.p.i., animals were anesthetized with isofluorane and brains were rapidly removed. Three hundred fifty μm horizontal olfactory bulb slices were cut with a Leica vibratome in cutting solution containing (in mM): 212 sucrose, 3 KCl, 1.25 NaH_2PO_4, 26 $NaHCO_3$, 7 $MgCl_2$, 0.5 $CaCl_2$, 10 glucose, and 310 mOsm, pH 7.3. Slices were recovered for 30 min at 32°C with recording solution containing (in mM): 125 NaCl, 2.5 KCl, 1.25 NaH_2PO_4, 26 $NaHCO_3$, 1 $MgCl_2$, 2 $CaCl_2$, 20 glucose, and 310 mOsm, pH 7.3 and continuously bubbled with carbogen. After recovery, slices were kept at RT.

Targeted whole-cell recordings were performed on GFP^+ nontruncated GCs with a MultiClamp700B amplifier (Axon Instruments) and pipette solution containing (in mM): 2 NaCl, 4 KCl, 130 K-gluconate, 10 Hepes, 0.2 EGTA, 4 ATP-Mg, 0.3 GFP-Tris, 14 phosphocreatine, 0.02 Alexa555 hydrazide, and 292 mOsm, pH 7.25. Pipette resistance was 6–9 MΩ. Access resistance was 12–30 MΩ, not compensated and regularly monitored during recordings. Liquid junction potential was not corrected. Data were acquired and analyzed with the pClamp9 software (Axon Instruments). Focal minimal stimulation of dendrites was performed with an A.M.P.I. Master-8 stimulator and a bipolar electrode inserted in a low-resistance patch pipette. Under fluorescence guidance, the stimulation electrode was positioned near a GFP^+ dendrite connected to the recorded cell. Recordings were performed at V_H = −70 mV close to the reversal potential of Cl^--mediated IPSCs. Focal stimulation was performed only in close proximity to a dendrite (<5 μm) and once evoked PSC was obtained, stimulation intensity was reduced, so that in most cases a failure rate of ≈50% was obtained and only a single-evoked PSC with short latency was evoked. Most evoked PSCs disappeared once the stimulation electrode was moved within a radius >5 μm. Recordings from the correct GCs were confirmed by colocalization of Alexa555 fluorescence with the GFP^+ GCs. Data from deep and superficial GCs were pooled, because they displayed similar kinetics and CTZ sensitivity. Cyclothiazide (CTZ, Sigma) was dissolved in DMSO.

Western Blot Analysis for PSD-95:GFP. Neurons were extracted with 80 μl SDS sample buffer per well and boiled for 10 min. The lysates (of the total) were separated by 10% SDS/PAGE and transferred onto nitrocellulose filters. The filters were incubated with a mouse antibody raised against PSD-95 (1:10,000, gift of M. Sheng) and were visualized by chemiluminescence. Cultures with >90% of neurons expressing PSD-95:GFP were used to compare endogenous and exogenous expression of PSD-95/PSD-95:GFP.

1. El-Husseini AE, Schnell E, Chetkovich DM, Nicoll RA, Bredt DS (2000) PSD-95 involvement in maturation of excitatory synapses. *Science* 290:1364–1368.
2. Schoppa NE (2006) AMPA/kainate receptors drive rapid output and precise synchrony in olfactory bulb granule cells. *J Neurosci* 26:12996–13006.
3. Balu R, Pressler RT, Strowbridge BW (2007) Multiple modes of synaptic excitation of olfactory bulb granule cells. *J Neurosci* 27:5621–5632.
4. Price JL, Powell TPS (1970) An electron-microscopic study of the termination of the afferent fibres to the olfactory bulb from the cerebral hemisphere. *J Cell Sci* 7:157–187.
5. Wellis DP, Kauer JS (1994) GABAergic and glutamatergic synaptic input to identified granule cells in salamander olfactory bulb. *J Physiol* 475:419–430.
6. Mori K (1987) Membrane and synaptic properties of identified neurons in the olfactory bulb. *Prog Neurobiol* 29:275–320.
7. Andreadis ST, Brott D, Fuller AO, Palsson BO (1997) Moloney murine leukemia virus-derived retroviral vectors decay intracellularly with a half-life in the range of 5.5 to 7.5 hours. *J Virol* 71:7541–7548.
8. Sanes JR (1989) Analysing cell lineage with a recombinant retrovirus. *Trends Neurosci* 12:21–28.
9. Kelsch W, Mosley CP, Lin CW, Lois C (2007) Distinct mammalian precursors are committed to generate neurons with defined dendritic projection patterns. *PloS Biol* 5:e300.

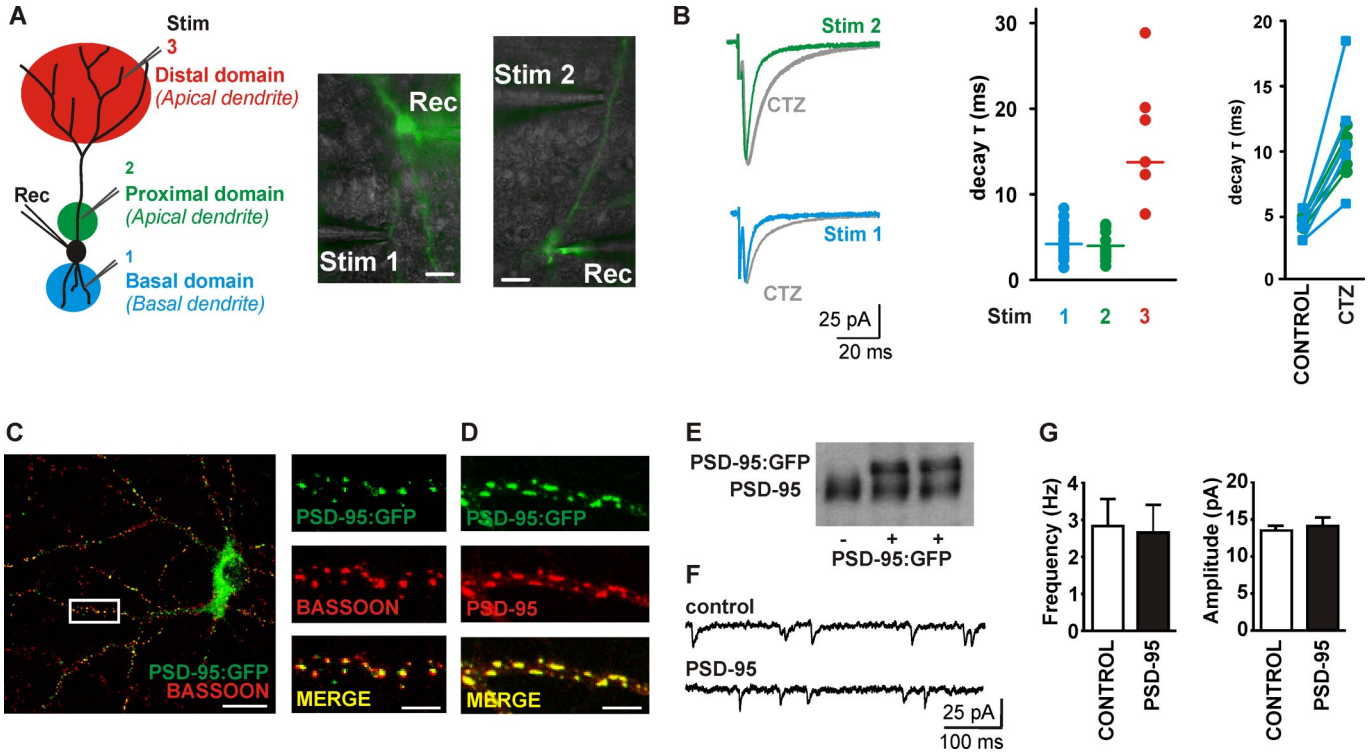

Fig. S1. Glutamatergic input to GCs in brain slices and functional properties of PSD-95:GFP expressed by a retroviral vector in cultured neurons. (*A Left*) Fluorescence guided focal low amplitude stimulation of one or few fibers terminating either at the basal (1), proximal (2), or distal domain (3). (*Right*) Sites of stimulation in close proximity to the respective dendritic domain (<5 μm) (Scale bar, 10 μm.) (*B Left*) Fluorescence guided focal low amplitude stimulation to activate one or few fibers terminating either at the basal (1) or proximal (2) domain evoked PSCs that were sensitive to the AMPA-receptor modulator CTZ (10 μM) ($V_H = -70$; both $n = 5$). (*Center*) Evoked PSCs at different dendritic domains (1, 2, or 3) with different 90–10% decay times recorded at $V_H = -70$ mV ($n =$ 18, 13 and 6, respectively). (*Right*) Graph shows change in 90–10% decay time in the same GC after application of CTZ for either the basal (blue) or proximal domain (green). (*C*) A cultured neuron was infected with PSD-95:GFP and labeled with antibody for Bassoon, a presynaptic protein. The confocal image revealed that PSD-95:GFP$^+$ clusters in dendrites were reliably contacted by a presynaptic terminal. The images on the *Right* are higher magnification (bar, 3 μm) of the box on the *Left* image (bar, 10 μm) showing PSD-95:GFP$^+$ clusters (*Top*), anti-bassoon immunofluorescence (*Middle*), and merged image (*Bottom*). All neurons were examined at 21 days in culture. (*D*) The PSD-95:GFP$^+$ clusters (*Top*) were found in all postsynaptic densities labeled by anti-PSD-95 immunofluorescence (*Middle*) as seen by the merged image (*Bottom*) (bar = 3 μm.) (*E*) The level of PSD-95 protein (95 kDa) expression was approximately doubled by viral expression of PSD-95:GFP (120 kDa) in cultured neurons 21 d.p.i. compared with the endogenous expression level. In the selected cultures, >90% of neurons expressed PSD-95:GFP. (*F*) Representative recordings of mEPSCs from two PSD-95:GFP-positive neurons 21 days after infection with a lentiviral vector and uninfected control cells from littermate cultures recorded at the same day (bars indicate 20 pA and 50 ms, respectively). (*G*) The graphs show the mean mEPSC frequency ($P = 0.84$) and amplitude ($P = 0.47$) of neurons infected with a lentiviral vector expressing PSD-95:GFP and uninfected control neurons ($n = 8$, respectively; all neurons were recorded at 21 d.p.i.).

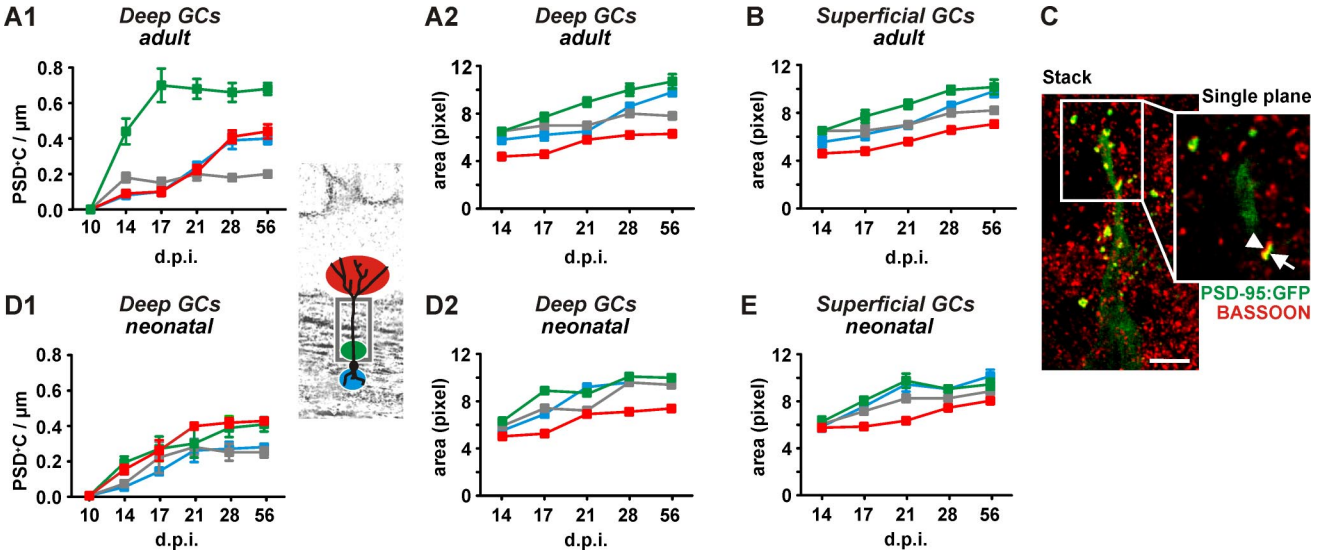

Fig. S2. Domain-specific development of PSD$^+$Cs during maturation of GCs (with branching in the deep or superficial external plexiform layer). (*A*) Mean PSD$^+$C density (*Left*) and mean PSD$^+$C area (*Right*) at different stages (d.p.i.) during the maturation of deep adult-generated GCs. The dendritic domains are indicated in the graphs: basal (blue), proximal (green) and distal domain (red) as well as the entire unbranched apical dendrite (gray). (*B*) Mean PSD$^+$C area at different stages (d.p.i.) during the maturation of superficial adult-generated GCs. (*C*) At 14 d.p.i., PSD$^+$Cs were regularly contacted by a presynaptic marker, bassoon, in adult-generated GCs (Scale bar, 5 μm.) (*D*) Mean PSD$^+$C density (*Left*) and mean PSD$^+$C area (*Right*) at different stages (d.p.i.) during the maturation of deep neonatal-generated GCs. (*E*) Mean PSD$^+$C area at different stages (d.p.i.) during the maturation of superficial neonatal-generated GCs.

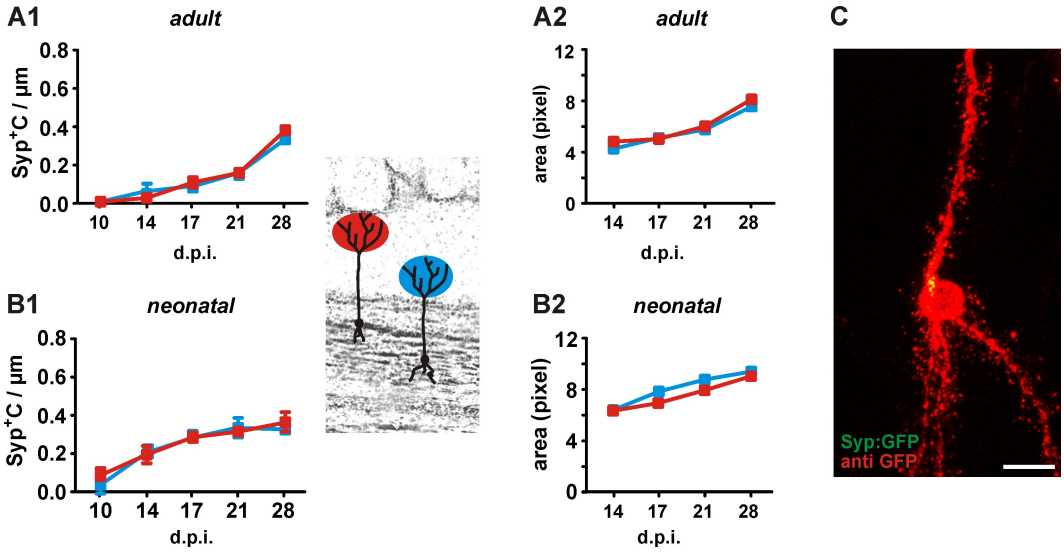

Fig. S3. Development of Syp$^+$Cs during maturation of GCs (with branching in the deep or superficial external plexiform layer). (*A*) Mean Syp$^+$C density (*Left*) and mean Syp$^+$C area (*Right*) at different stages (d.p.i.) during the maturation of deep (blue) and superficial (red) adult-generated GCs. (*B*) Mean Syp$^+$C density (*Left*) and mean Syp$^+$C area (*Right*) at different stages (d.p.i.) during the maturation of deep (blue) and superficial (red) neonatal-generated GCs. (*C*) No Syp$^+$Cs were detected at the basal and proximal domain in an adult-generated GC (28 d.p.i.; Scale bar, 10 μm.)

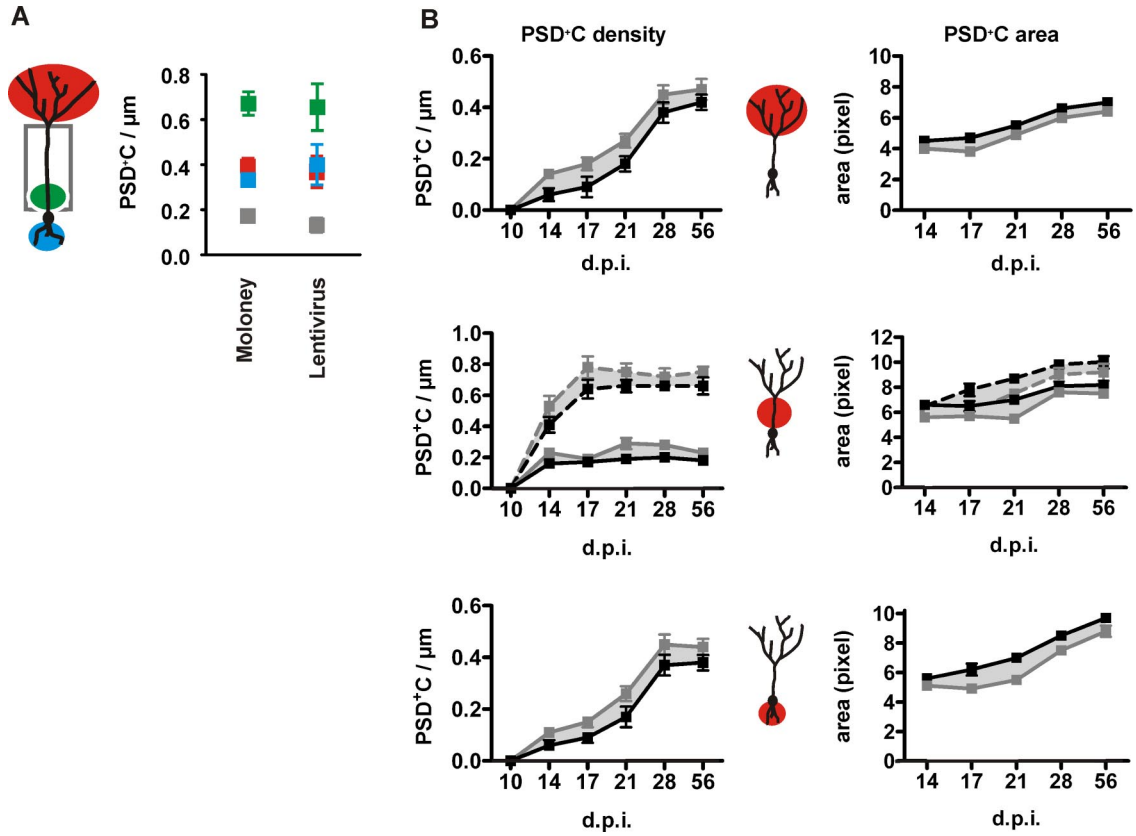

Fig. S4. The domain-specific development of PSD$^+$Cs is independent of their thresholding. (*A*) Comparison of PSD$^+$C density for adult-generated GCs for expression with a lentiviral vector HsynPSD95g (used for *in vitro* testing) and oncoretroviral vector MRSVPSD95g (used for birthdating of the new neurons and subsequent study of maturation of GCs). The dendritic domains are indicated in the graphs: basal (blue), proximal (green) and distal domain (red) as well as the entire unbranched apical dendrite (gray). (*B*) Development of PSD$^+$Cs during maturation of adult-generated superficial GCs at the different time points indicated (in d.p.i.). To determine whether the late appearance of PSD$^+$Cs at the basal and distal domains was because of setting a threshold for PSD$^+$Cs used throughout this study (≥ 3 adjacent pixels was considered a cluster), we compared our data to a lower threshold setting (≥ 2 adjacent pixels was considered a cluster)—but might therefore also include more noise. With setting a lower threshold (gray lines), the absolute PSD$^+$Cs density was slightly higher, but the pattern of PSD$^+$C development persisted, compared with thresholding used throughout this study (black lines), and was therefore not because of differences in PSD$^+$C area in the respective dendritic domain. In the *Middle* graphs the dashed lines represent the proximal domain and the continuous line the entire unbranched apical dendrite. Mean PSD$^+$C density (*Left* images) and mean PSD$^+$C area (*Right* images).